ON THE STRING-BRIDGE INTERACTION IN INSTRUMENTS WITH A ONE-SIDED (BRIDGE) CONSTRAINT

Knut Guettler
Norwegian Academy of Music
P.B. 5190 Majorstuen, 0302 Oslo, Norway
knut.guettler@nmh.no

ABSTRACT
Certain Indian instruments, like the tanpura, vina, and sitar, are designed in such a way that the string regularly hits a part of the elongated bridge, some millimetres away from the string's fixed end. The bridge thus interferes with the natural movement of the plucked string, and drastically changes its wave pattern and energy content. Different instruments of this kind are equipped with differently shaped bridges, partly dependent on whether the string is meant to be pressed down on a fret or not. When frets are utilized, the bridge profile must allow for changes in the string angle without introducing noticeable differences in the string-bridge gap. The present analyses are based on computer modelling of such interaction with a variety of bridge profiles. Four main types of bridge profiles were investigated: (1) Flat, with the string touching the entire bridge length when at rest; (2) Pointed, like a crossing fret, where the bridge obstructs the string's movement in one point only. (3) Roof shaped, with the string touching the bridge in a single point when at rest, and a greater part of the bridge when the string amplitude surpasses a certain value; (4) Curved, with the string touching the bridge tangentially; The two last profiles produce a string-corner rotation resembling the one seen in bowed strings during Helmholtz motion − this to some degree leads to a sawtooth-like force pattern on the bridge, like in bowed instruments. The other two profiles cause normally no such corner rotation, and the resulting force on the bridge is composed of a series of pulses. However, the second, single-point profile, seems superior when it comes to preserving the string energy. In all cases the string vibrates with a frequency slightly higher than when vibrating in its natural mode free from obstructions. This difference in modes is one of the reasons why even-numbered harmonics are present, even when the string is excited at its midpoint (apparently violating Young-Helmholtz's law). The fact that the bridge is driven not only at the string's end point, but over several millimetres of its length makes the driving force take rather unique patterns. Here it can be seen that although the general outline may be repeating from period to period, small aperiodicities interfere at all times, giving the sound more "life" than would otherwise be the case.

THE FLAT CONSTRAINING BRIDGE (BRG 1 AND BRG 2)

The bridge BRG 1 is 20 cm long, flat, and its height in line with the string's equilibrium. This is certainly a bridge that is not commonly used, but we introduce it here to serve as a vehicle for understanding some basic principles of the string-bridge interaction. In Figure 1 the bridge BRG 1 is occupying no less than one fifth of the string length, its size chosen to make transients short so that we can easily overlook the development. For all computer simulations the following string parameters were used: The string is ideal (i.e., totally flexible and with no internal damping) and has a length of 1 m; point of excitation, 0.5 m from terminations (i.e., at the string midpoint); fundamental frequency of the unconstrained string, 100 Hz; initial amplitude, 5 mm. The system has no losses, i.e., perfect reflections everywhere. For the graphs, the string's position and velocity are recorded at the point of excitation. The force shown is the force acting on the bridge, integrated over the entire bridge length (the bridge considered incompliant).

After release at time zero (i.e., $t = 0$), the string travels freely until it hits the bridge after 2.5 ms – or one fourth of the nominal period (i.e., T/4). At that time a part of the string makes an impact

on the entire bridge length, whereafter it immediately moves up again, eventually forming a triangle with the apex above the bridge midpoint, that is 10 cm from the string termination (or the "jwari thread", if you like). The impact on the bridge is impulsive, and covering its entire length. The string makes an instant rebound, but returns to repeat its impact one millisecond after the first one. This local cycle goes on until the part of the string just outside the bridge returns on its way back (i.e., at $t = 6.5$ ms). On its way up above its equilibrium line, the string is taking a shape different from the straight line it had on its way down (see the arrows in the string diagram). As can be seen from the position plot, the string (at its point of excitation) never reaches the initial amplitude of 5 mm, but a mere 4.5 mm at $t = 0.9$ T.

When regarding the force signal of Figure 1, one sees a series of negative impulses with a positive offset caused by the upwards pull of the string. (Computationally it gives no meaning to specify the magnitudes of these impulses as these occupy one time step each and magnitudes hence will increase with the time-domain resolution. Impulses are therefore dashed.) The impulse pattern consists of four impulses 0.1 T apart—their sequence initially repeating each 0.9 T—in addition to a "moving" impulse starting at $t = 0.65$ T, and repeating with somewhat longer intervals. Except for the time points of the impacts, the string is not touching the bridge. Even though impulse magnitudes are meaningless, the ratio between them is not. As can be seen, the moving impulse is only ¾ of the stationary ones, the reason being that at that time the string is hitting only the innermost ¾ of the bridge. In the model the bridge is completely stiff. In practice, the bridge material will drastically influence the buildup of impulses.

Notice in the uppermost panel, the string segments to which the arrows are pointing. They describe the shape of the string when returning after 0.8 T (long arrow) and 0.85 T (short arrow), respectively. The string is not returning to its initial shape.

For comparison we shall repeat the simulation with another bridge adjustment, BRG 2 (see Figure 2). Here the same flat bridge is moved one millimetre down below the string's equilibrium. With this adjustment we get a series of negative *pulses*, offset by the same initial upwards pulling force of the string. We also get *im*pulses in the middle of most of the pulses. The pulses are formed when the string is on its way down to the bridge, after passing equilibrium. Only half the bridge length is impacted by the string with BRG 2, and we notice that the number of impulses is reduced to three (the interval between them being 0.15 T), simply because the wave top of the string segment above the bridge travels a longer distance: diagonally from the rightmost corner of the bridge to a point 0.5 mm above the bridge, and back (see dotted line); 1.5 mm height in total. In BRG 1 the wave top travelled 1.0 mm up and down between impulses. For any negative *pulse* to occur, the bridge must of course be positioned lower than the line of equilibrium. Another interesting difference between BRG 1 and BRG 2 can be seen in the string velocity signal. While the string at its midpoint made a series of stops with BRG 1, it flows continuously with BRG 2. The "moving impulse" of BRG 1 has become a moving *pulse* with the adjustment of BRG 2. The lowering of the bridge has increased the effective period at the onset (interval between each series of triple pulses) to 0.95 T, while the moving pulse gets an interval closer to the nominal period. Notice that the two string profiles in the uppermost panel (also here recorded at 0.80 T and 0.85 T, respectively) have advanced slightly less for BRG 2 than ditto for BRG 1.

THE POINTED BRIDGE (BRG 3 AND BRG 4)
A pointed bridge is more realistic than the flat one, and has been investigated by C. Cuesta et al[1]. We shall for comparison, however, repeat the analyses we did for BRG 1 and 2: Regard the force pattern of BRG 3 in Figure 3. Here we got *two* negative pulses repeated in cycles with effective

period of 0.9 T. That is, for four periods, after which one period follows with duration of only 0.8 T. The whole sequence then repeats. A "wandering" pulse can also be seen, initially repeating with period equal to the nominal period, 1.0 T. Its presence obviously interferes with the two, more stable pulses. In general, the wave pattern repeats itself with a sequence of five periods not all of equal length.

For BRG 4 (see Figure 4), were the pointed bridge is lowered to 1.0 mm below the equilibrium line, the corresponding initial pulse periods are seen to be 0.95 T and 1.0 T, respectively. The "extra" negative pulses that are superimposed on the ones of lesser magnitude, are caused by the string folding over the pointed bridge (see the lower dashed line of the string diagram of Figure 4). Apparently this bridge functions well, as has been shown by ref. 1, but as we see: with a perfectly flexible string, it does not create a sawtooth force pattern, as do some other bridge profiles.

THE ROOF-SHAPED BRIDGE (BRG 5 AND BRG 6)

Figure 5 displays the effects of a roof-shaped bridge: The bridge is 200 mm wide, symmetrical, and its edges positioned 0.5 mm below the string's equilibrium, both at the free side of the string and the fixed end, i.e., where a jwari thread would be placed. The bridge top (the "ridge") is inline with the string's equilibrium, at 0.0 mm. The velocity and force signals display a rather noisy system, the effective periods more and more dominated by pulses or impulses. Compared to BRG 5, the signals of BRG 6 (see Figure 6) looks considerably more organized, and the string's amplitudes do not by far decay as rapidly as in Figure 5. However, the difference in profile of the two bridges is rather small: BRG 6 has the same alignment of its top as BRG 5, but its sides are slightly steeper: The bridge edges are 0.8 mm below the equilibration line, giving a difference between the two bridges of a mere 0.03 mm per centimetre string/bridge length.

However, when analysing this difference more closely, one quickly realizes its significance: As the string is released, a progressively longer piece of the string is moving downwards toward the bridge with a constant velocity (here, −200 cm/s). When reaching equilibrium, the entire string is moving with this speed, as indicated by the downward arrows in the uppermost panel. Just before the impact, the string velocity can thus be described quite simply as

$$\frac{\delta y_{STR}}{\delta x} = 0; \qquad \frac{\delta y_{STR}}{\delta t_-} = \alpha = -2 \text{ m/s}, \tag{1}$$

while the right side slope of the bridge, BRG 5, can be described as

$$\frac{\delta y_{BRG}}{\delta x} = \psi = -5 \times 10^{-3}. \tag{2}$$

The string's particle velocity immediately after its (particle) impact on the bridge can furthermore be expressed in the following simple form:

$$\frac{\delta y}{\delta t_+} = -\alpha + \text{sgn}(\alpha)|\psi| c, \qquad (|\alpha| \geq |\psi| c), \tag{3}$$

where c is the wave propagation speed (here, 200 m/s).

With the present parameters, this gives a particle (rebounded) velocity for BRG 5 and BRG 6 of 100 and 40 cm/s, respectively. With a slope of −1.0×10⁻² or steeper (the magnitude equal to or

greater than the string's initial slope) there would be no reflection, and the bridge would act as a single-point constraint unless the initial string amplitude be increased. This also implies that the roof-shaped bridges act as single-point bridges in the last part of the tone when realistically damped strings are being played.

One important difference between bridges BRG 5 and BRG 6, and the previous ones, is that these bridges start shaping the string in a manner that could eventually lead to Helmholtz-motion-like movement of the string. That is: one corner rotating (anti-clockwise in the figure) with otherwise relatively straight string segments. Such a rotation would form a sawtooth force signal on the bridge, which to a large degree characterizes the sound of bowed instruments. When I first time listened to the tanpura, this quality was the first thing that struck me (being a string player…). Regard our snapshots of the string forms, taken at $t = 0.8$ T and 0.85 T as usual: For both bridges the string has, at the conclusion of the first period, taken a slightly rounded, but more importantly: *tilted*, profile. The characteristic kinks that were created with the previous bridges are completely missing here. Only one is seen (marked with outside arrows on the right side of the envelope).

THE CIRCULARLY ROUNDED BRIDGE (BRG 7, BRG 8, BRG 9)
The profile of bridge BRG7 is formed as a circle segment, where the slope of the bridge at $x = 0$ (i.e., just under the string end) is equal to the initial slope of the string when drawn up 5 mm at its midpoint. To calculate the radius of this circle, the following equation may be used:

$$a = \frac{L_{BRG}}{2}\sqrt{1 + \left(\frac{\delta y_{STR}}{\delta x}\right)^{-2}} \tag{4}$$

where L_{BRG} is the distance from the string end to the outermost point where the string will be touching the bridge—and the parenthesis contains the initial slope of the string. In the present case, BRG 7 and BRG 8—with the bridge top point placed 100 mm from the string end—the radius, a, amounts to 10 m, and for BRG 9, twice as much.
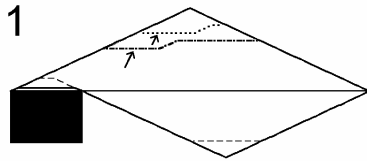
The height of this segment above the outermost touching point can furthermore be calculated as

$$h = a\left[1 - \sin\left(arc\cot\left(\frac{dy_{STR}}{dx}\right)\right)\right]. \tag{5}$$

For both BRG7 and BRG 8 this value is 0.5 mm. However, for BRG 7 the bridge top is aligned with the string's equilibrium line, while for BRG 8 *the outermost touching point* (i.e., the bridge edge at $x = 200$ mm) *is aligned with the same line* (see Figures 7 and 8). Here the string-movement diagram clearly shows that in both cases only one corner is created, indicating a Helmholtz-like corner rotation. Anyhow, BRG 8 appears as the most successful one as far as maintaining energy is concerned.

For BRG 9 the bridge diameter is doubled, and the circle segment's top point moved to the jwari position. The resulting signals resembles those of BRG 8 in many respects, but for BRG 9, which initially is not in touch with the string, the bridge-force pattern shows a positive pulse of decreasing width, after a negative sawtooth. Here too, only one string corner is created, indicating a development towards Helmholtz motion.

BRG 1

Bridge properties:
Flat, 200 mm long,
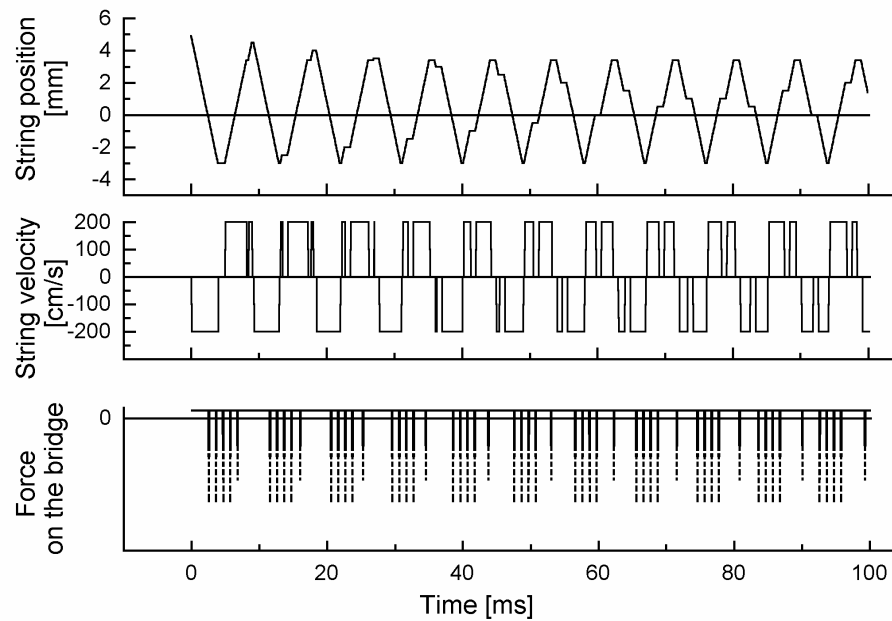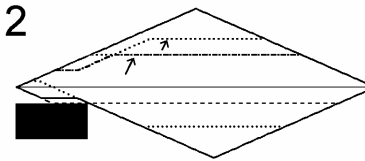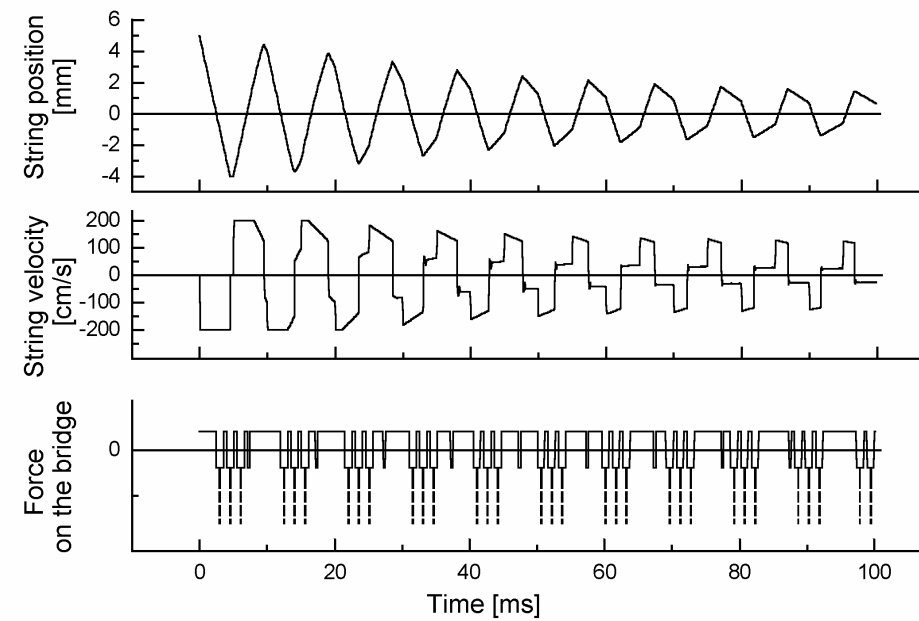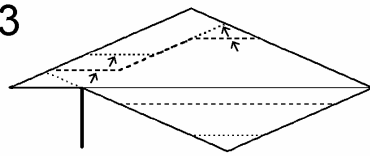0.0 mm below string equilibrium

Figure 1: Signals obtained with a flat bridge, 200 mm long (occupying 1/5 of the string length). Alignment: string equilibrium. Except for the offset caused by the initial string angle, only impulses are seen in the force signal. The two arrows in the upper panel point at the string shape at $t = 0.8$ T and 0.85 T, respectively, i.e., when the string is returning to a shape close to its initial shape.

BRG 2

Bridge properties:
Flat, 200 mm long,
1.0 mm below string equilibrium

Figure 2: Signals obtained with a flat bridge, 200 mm long (occupying 1/5 of the string length. Alignment: 1.0 mm below string equilibrium. A combination of pulses and impulses are seen in the force signal when the bridge is lowered with respect to the string's equilibrium line. The arrows are pointing at the string shape at $t = 0.8$ T and 0.85 T, respectively.

BRG 3

Bridge properties:
Pointed, 200 mm away from end,
0.0 mm below string equilibrium

BRG 4

Bridge properties:
Pointed, 200 mm away from end,
1.0 mm below string equilibrium

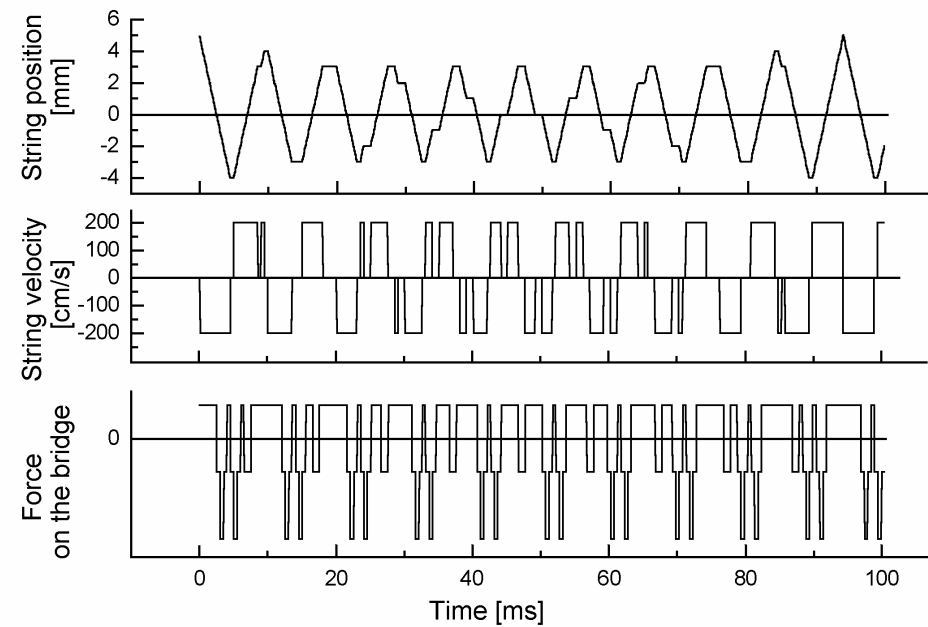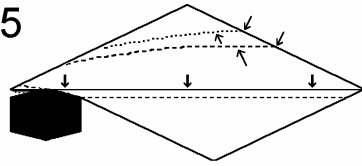**Figure 3:** Signals obtained with a single-point bridge, 200 mm away from the string end (i.e., 1/5 of the string length). Alignment: string equilibrium. Except for the offset caused by the initial string angle, only negative pulses are seen in the force signal. The two arrows point at the string shape at $t = 0.8$ T and 0.85 T, respectively. The pulse sequence is repeating every 4.4 T.

Figure 4: Signals obtained with a single-point bridge, 200 mm away from the string end (i.e., 1/5 of the string length). Alignment: 1.0 mm below string equilibrium. The initial effective period has increased, and so has the interval between repeating sequences. The arrows are pointing at the string shape at $t = 0.8$ T and 0.85 T, respectively.
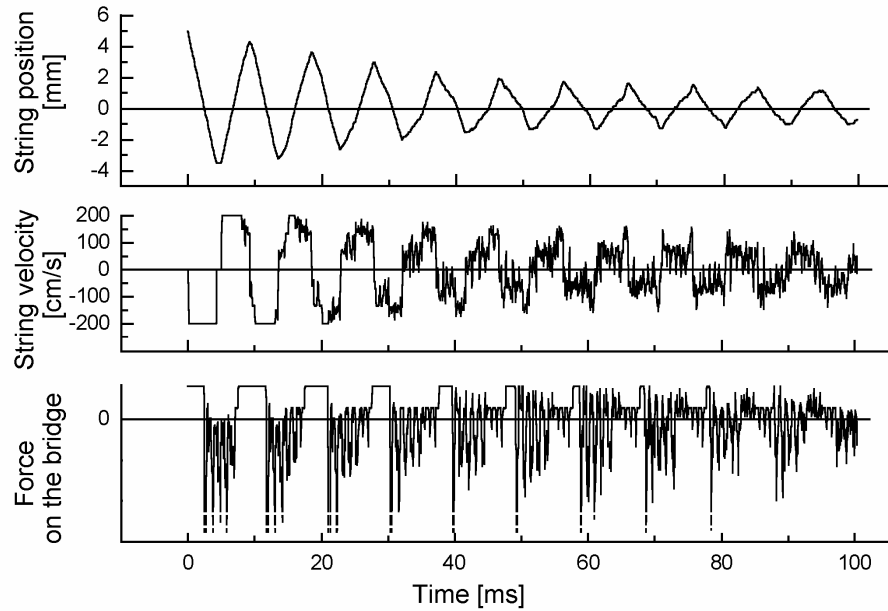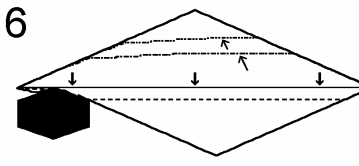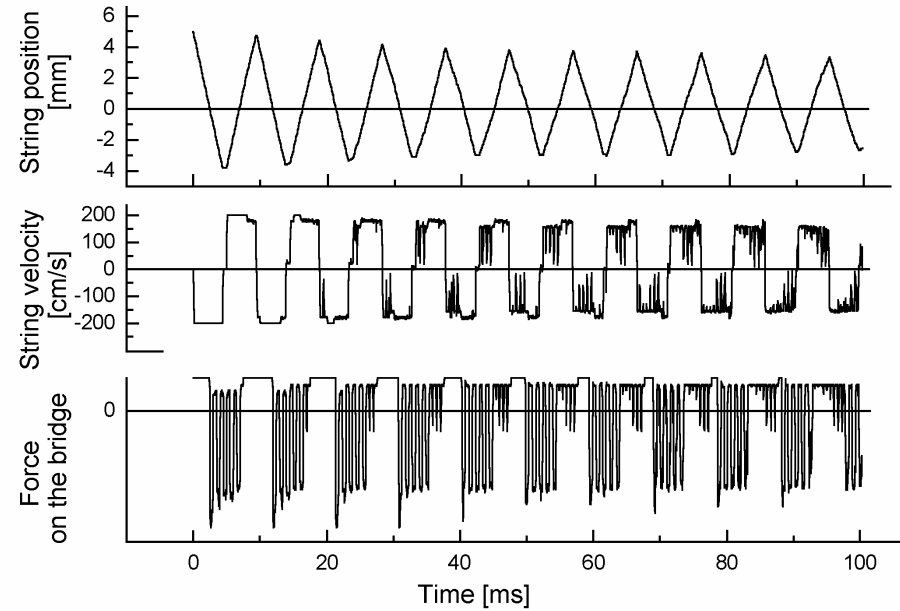
Figure 5: Signals obtained with a symmetrical roof-shaped bridge, 200 mm wide (occupying 1/5 of the string length), with its top point 100 mm away from the string end. Alignment of top point: in line with string equilibrium. Except for the offset caused by the initial string angle, mainly impulses are seen in the force signal. The two arrows in the upper panel point at the string shape at $t = 0.8$ T and 0.85 T, respectively. Notice that the string at that time has taken a tilted and partly rounded shape with only one distinct corner, to which the arrows are pointing from outside the string envelope.
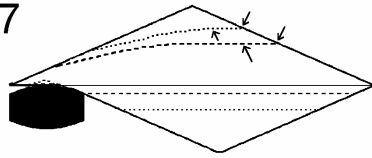
Figure 6: Signals obtained with a symmetrical roof-shaped bridge, 200 mm wide (occupying 1/5 of the string length), with its top point 100 mm away from the string end. Alignment of top point: 1.0 mm below the string equilibrium. Except for the offset caused by the initial string angle, mainly impulses are seen in the force signal. The two arrows point at the string shape at $t = 0.8$ T and 0.85 T, respectively. Notice that the string has taken a slightly tilted shape, but there still exists one corner on each side of this segment.

BRG 7

Bridge properties:
Circular segment, symmetrical,
200 mm wide,
top 0.0 mm below string equilibrium

BRG 8

Bridge properties:
Circular segment, symmetrical
200 mm wide,
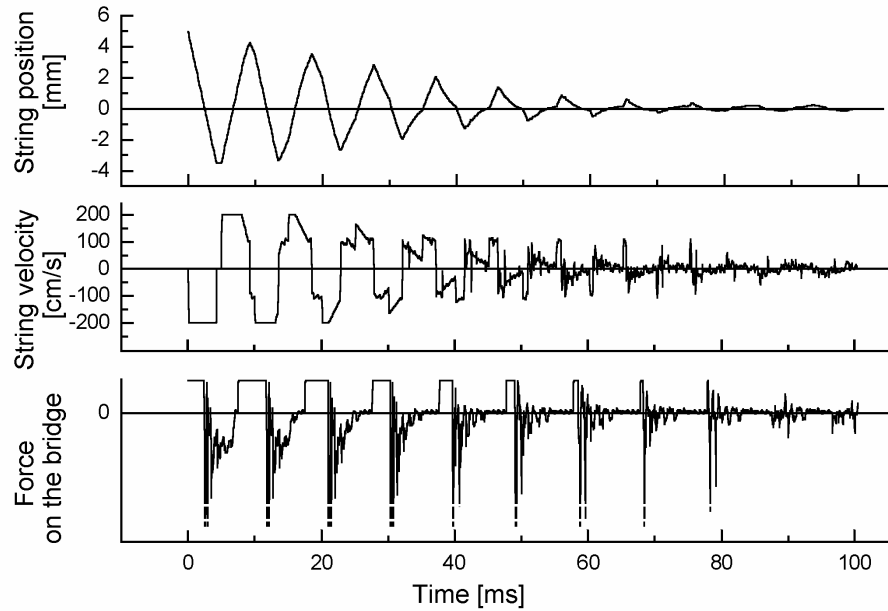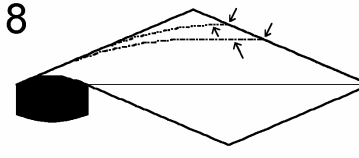top 0.5 mm above string equilibrium

Figure 7 Signals obtained with a circular bridge with diameter 10 m, from which a segment of length 200 mm is derived. Alignment: string equilibrium. Except for the offset caused by the initial string angle, mainly impulses are seen in the force signal. The arrows point at the string shape at t = 0.8 T and 0.85 T, respectively. As can be seen, only one corner exists, a sign of the creation of a rotating Helmholtz corner. However, the whole pattern falls together when the positive "square pulse", seen in the force signal, is reduced to nothing after 6 – 8 nominal periods.
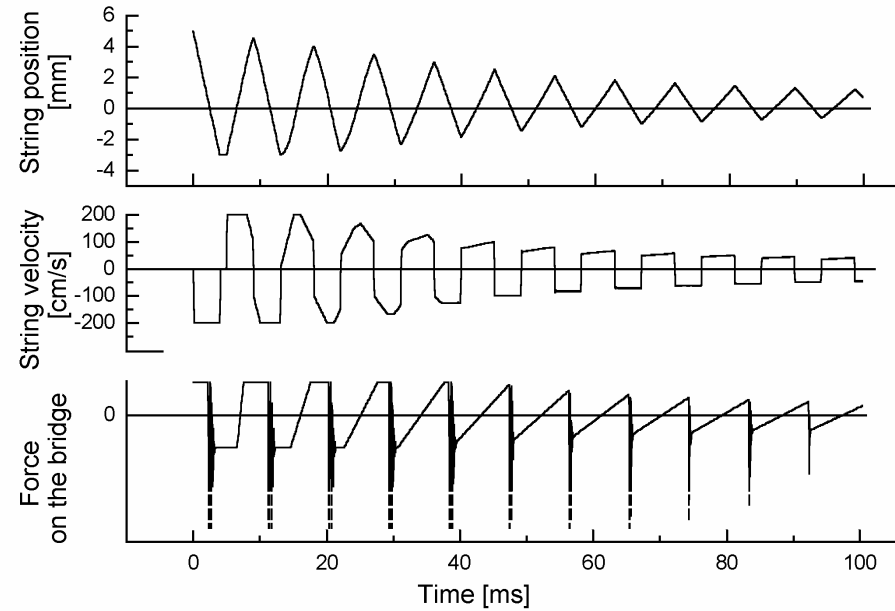
Figure 8: Signals obtained with a circular bridge with diameter 10 m, from which a segment of length 200 mm is derived. Alignment: 1.0 mm below string equilibrium. A combination of pulses and impulses are seen in the force signal when the bridge is lowered with respect to the string's equilibrium line. Compared to BRG 7, the positive force pulses are not vanishing: only changing form from square to triangular. A very noticeable reduction of the string amplitude can be seen, however.
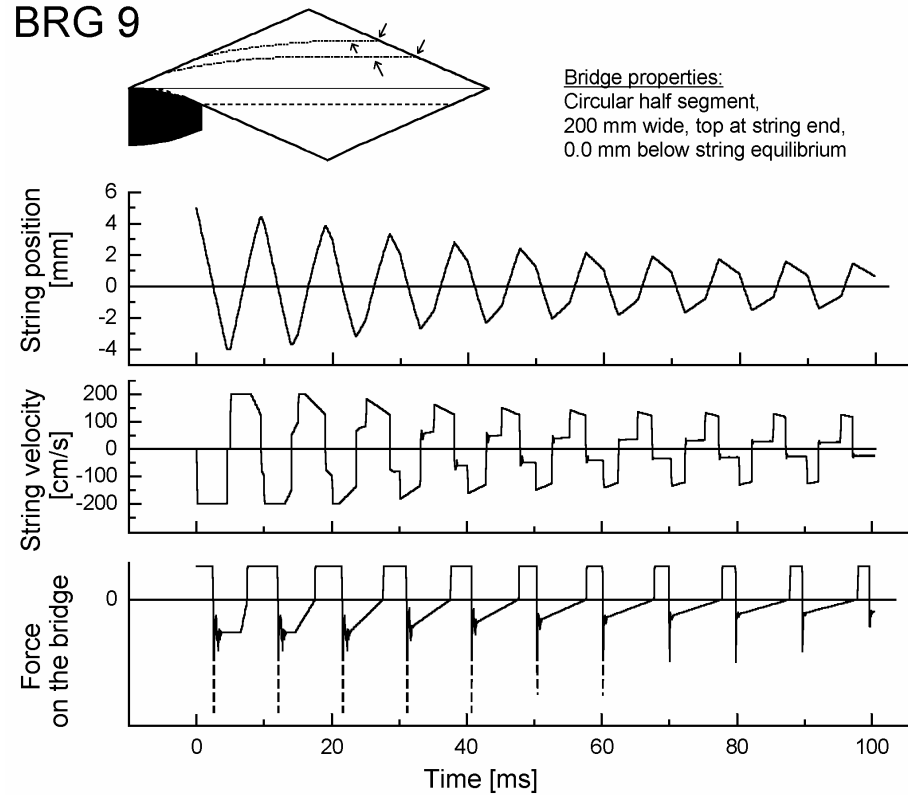
Figure 9: Signals obtained with a circular bridge with diameter 20 m, from which a *half* segment of length 200 mm is derived. Alignment: string equilibrium. The force signal has some similarities with ditto in BRG 7, but most of the impulses have gone. However, in contrast to BRG 8, where a triangular pulse was quickly created in the force signal, also positive pulses of decreasing widths can be seen. In the upper string diagram, the two arrows point at the string shape at $t = 0.8$ T and 0.85 T, respectively, where the creation of a Helmholtz corner can be seen.
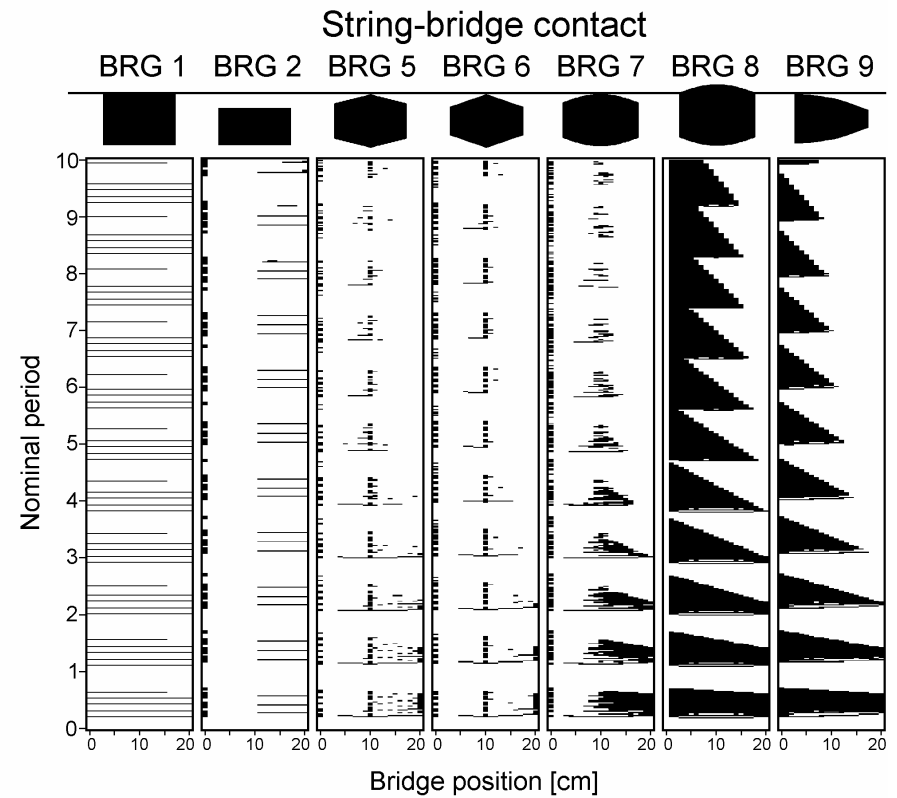
Figure 10: Time space diagram indicating contact between the string and the bridge. Black indicates downward force on the bridge surface. The leftmost fringe in each diagram represents the force on the jwari thread. Notice how BRG 8 and BRG 9 differ substantially from the other bridges in that the string keeps in contact with the bridge most of the time, covering a large part of its length. The step-like pattern in these diagrams are artefacts due to the modest graphic resolution in the bridge's length direction (10 mm), chosen for printing clarity.

SCALING DOWN TO REALISTIC BRIDGE DIMENSIONS

The bridges utilized for analyses so far have been about 20 times bigger than realistic bridges, for which a top point might be only some 5 mm away from the jwari thread or string end. Scaling down to realistic dimensions imply a few necessary modifications of our model: The resonances between the bridge top and the jwari thread would take extremely high frequencies that would quickly be damped by a soft thread. It should hence be realistic to lowpass all resonances at this string end. Furthermore, some damping of the string on the nut side of the bridge should also be needed. Simulating with bridges scaled down from BRG 1 through BRG 9, while implementing the above conditions, confirm qualitatively the transients shown in Figures 1 through 9, although with a significantly slower pace. Still, only the scaled-down copies of BRG 7 through BRG 9 will produce the Helmholtz pattern (albeit not always perfectly), while the other bridges tend to produce a force signal of a rounded square wave, rather than the sawtooth. But: two spectral features are very visible: (1) Even-harmonics build up in all cases (2) No formant can be seen, let alone their downward shifts, provided the string possesses ideal flexibility. The latter characteristic seems indeed related to the dispersive nature of realistically stiff strings (as stated by Cuesta et al. in ref 1). When implementing dispersion in our simulation model, the downward formant shifts consequently become quite apparent. Technically this implementation is done by introducing a low-pass filtered Airy function as our reflection function by the nut[2]. See Figure 11. This function returns high frequencies earlier than lower ones, causing a "ringing" high-frequency buildup in the system, discussed in ref 1. As these frequencies diminish with time due to natural damping, lower frequencies take consistently over as the dominating range.

CONCLUSIONS

Four shapes of bridges were investigated with respect to their effect on the string movement by use of computer simulations. In all cases even harmonics developed. Only rounded bridges gave string movements with one rotating corner, as described by Burridge et al[3]. However, a string possessing a certain *stiffness* would probably itself introduce some rounding when hitting a pointed top on a narrow bridge. If so, it would be more correct to say that a pointed bridge practically acts much like a rounded bridge, than vice versa, as was stated in ref. 1, pp 202. Formants and their spectral shifts were only visible when modelling with wave dispersion.
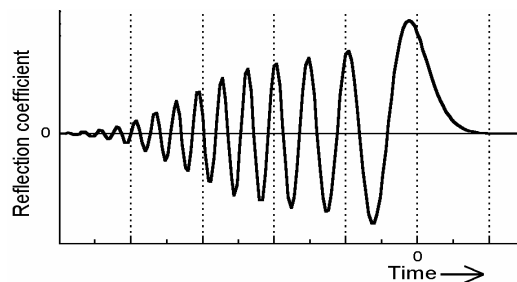

Figure 11: Lowpass-filtered Airy function used as reflection function to introduce frequency dispersion. The integral of this function is unity. (See ref. 2.)
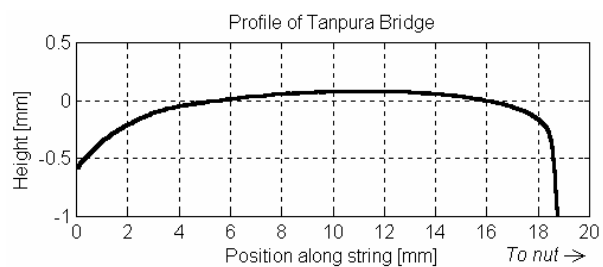

Figure 12: Real tanpura bridge measured with high resolution, and averaged over 5 string courses. The jwari thread would most likely be positioned somewhere on the bridge between 3 and 7 mm.

REFERENCES

[1] Cuesta, C., et al. "The tampura bridge as a precursive wave generator" (1991) *Acustica* 74, pp 201 208.

[2] Woodhouse, J., "On the playability of violins. Part I: Reflection functions" (1993) *Acustica* 78, pp 125-136.

[3] Burridge, R., et al. "The sitar string, a vibrating string with a one-sided inelastic constraint" (1982) *SIAM J. Appl. Math.* Vol. 42, No. 6. pp 1231-1251.